Fluemann et al., Supplementary Fig. S1

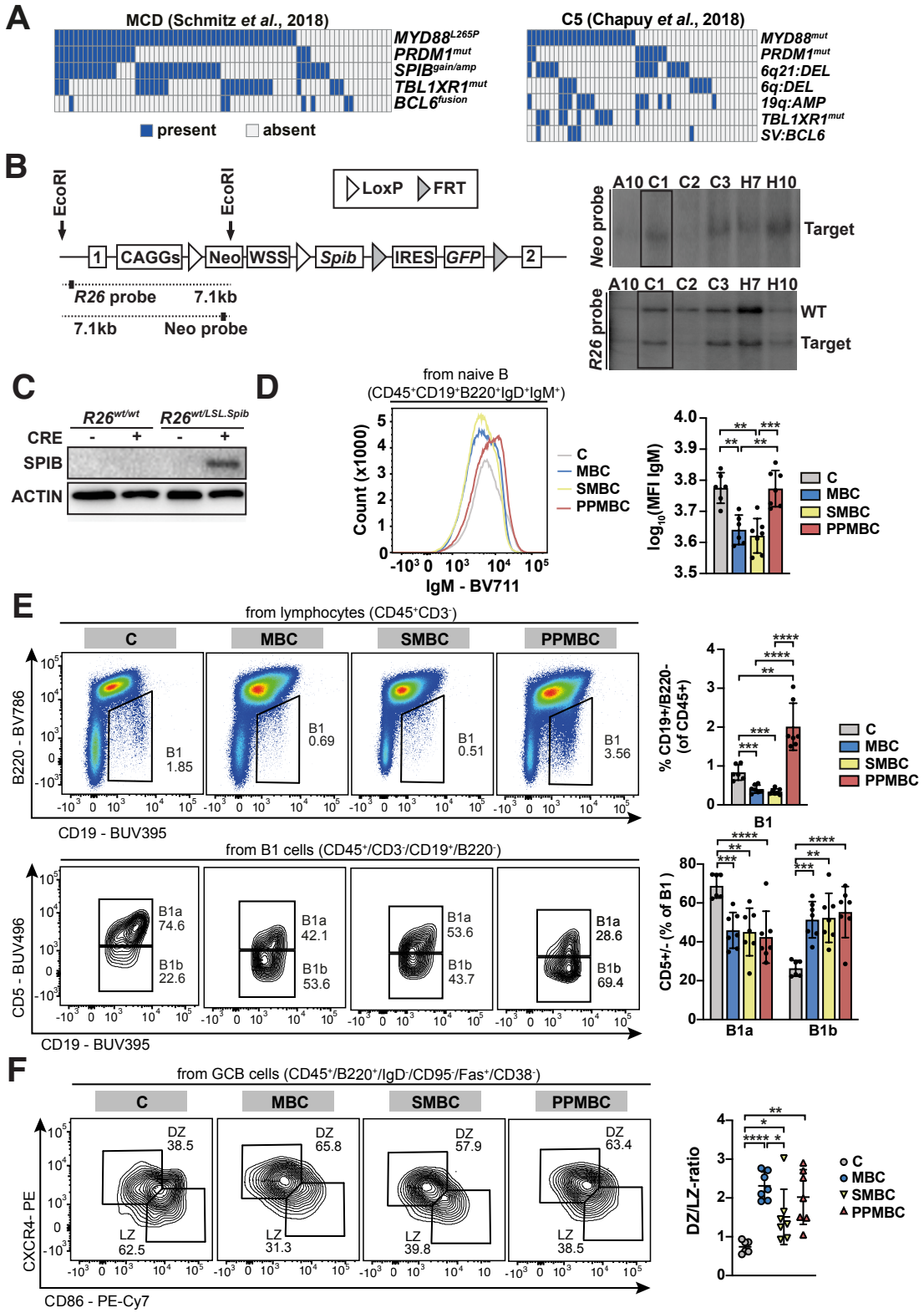

Supplementary Figure S1. (A) Analysis of published datasets for the co-occurrence of *MYD88* mutations and *SPIB/PRDM1* mutations as well as chromosomal aberrations

affecting the locations of *PRDM1/SPIB* in the DLBCL clusters C5/MCD. **(B)** Targeting of the *Rosa26* locus in C57BL/6J ES cells. The *Rosa26* locus was targeted with the linearized vector as described before (19, 20) and the targeted allele is schematically depicted (left panel). Murine *Spib* cDNA expression is controlled by a *CAGGs* promoter and prevented by a *lox*-stop-*lox* cassette. *GFP* expression is coupled to *Spib* expression by an internal ribosomal entry site (IRES). The Southern blots of EcoRI digested genomic DNA probed with a *R26* and a *Neo* probe, respectively, are shown (right panel). Positions of restriction sites and probes are shown in the schematic drawing above. **(C)** $Rosa26^{wt/wt}$ and $Rosa26^{wt/LSL.Spib}$ MEFs were transduced with AdenoCre. Cells were lysed, proteins were separated on SDS-PAGE, and SPIB was visualized by immunoblot. **(D)** Splenocytes of 10 weeks old C (n = 6), MBC, SMBC and PPMBC (n = 7 each) were analyzed by flow cytometry and the mean fluorescence intensity (MFI) of IgM was determined on naïve B cells. Representative histograms (left panel) and quantification (right panel) are depicted. **(E)** The frequency of B1 cells in spleens of 10 weeks old C (n = 6), MBC, SMBC and PPMBC mice (n = 7 each) was determined by flow cytometry, as well as the fraction of B1a and B1b cells. **(F)** Quantification of the dark zone/light zone ratio within the GCB population of 10 weeks old C (n = 6), MBC, SMBC and PPMBC mice (n = 7 each). *, $p \leq 0.05$; **, $p \leq 0.01$; ***, $p \leq 0.001$; Welch's unpaired two-tailed t-test; error bars represent SD.

Fluemann et al., Supplementary Fig. S2

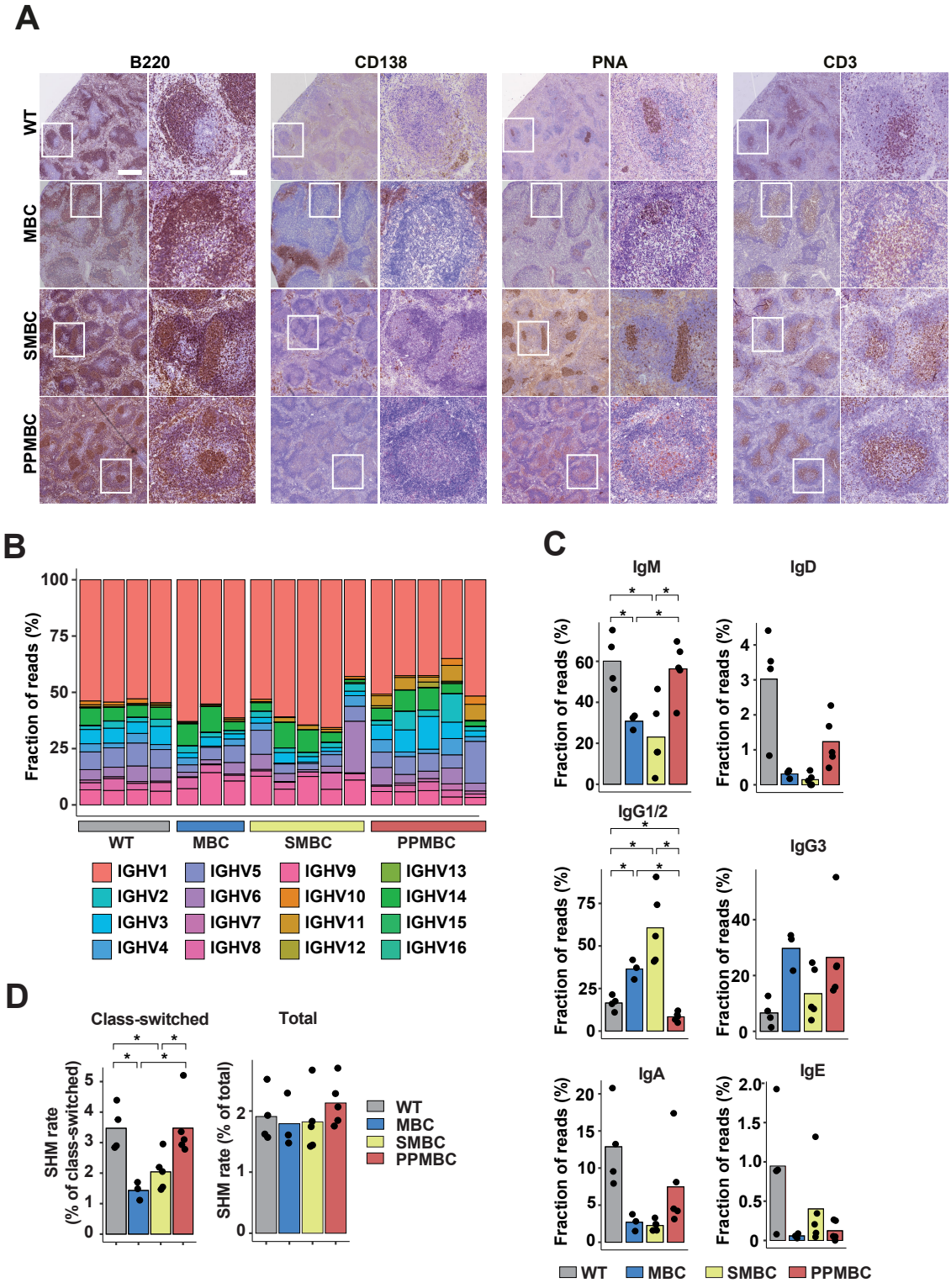

Supplementary Figure S2. (A) Representative immunohistochemical stainings of germinal center structures of WT (n = 10), MBC, SMBC and PPMBC animals (n = 5

each). Scale bars represent 500 µm and 100 µm (low and high magnification, respectively). Quantifications are illustrated in **Fig. 1F**. **(B)** The BCR repertoires of PNA^{pos} cells isolated from spleens of 10 weeks old WT (n = 4), MBC (n = 3), SMBC (n = 5) and PPMBC (n = 5) animals were sequenced and the frequencies of IGHV family usage were assessed. A detailed statistical analysis can be found in **Tab. S1**. **(C)** Fraction of reads mapped to the individual isotypes for each genotype. **(D)** The SHM rate for either class-switched sequences (of IgG1/2, IgG3, IgE, IgA isotypes) or all sequences (IgD, IgM, IgG1/2, IgG3, IgE, IgA) is depicted. *, $p \leq 0.05$; **, $p \leq 0.01$; ***, $p \leq 0.001$; Welch's unpaired two-tailed t-test; error bars represent SD.

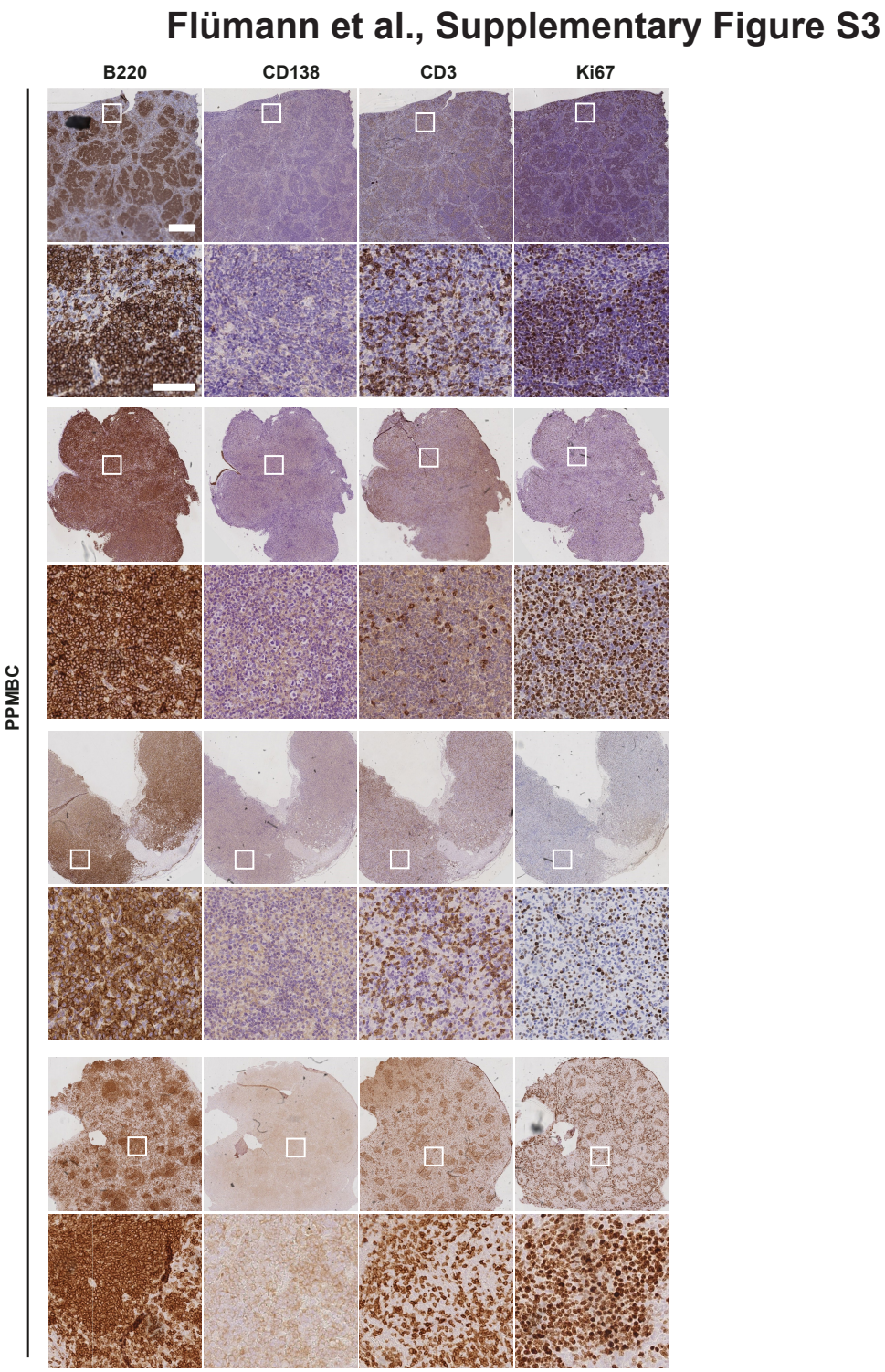

Supplementary Figure S3. Four representative IHC stainings of the analysed PPMBC tumors (n = 24). The displayed staining patterns serve to illustrate the morphological and immunohistochemical bandwidth of PPMBC lymphomas. Scale bars represent 1000 µm and 100 µm (low and high magnification, respectively).

Flümann et al., Supplementary Figure S4

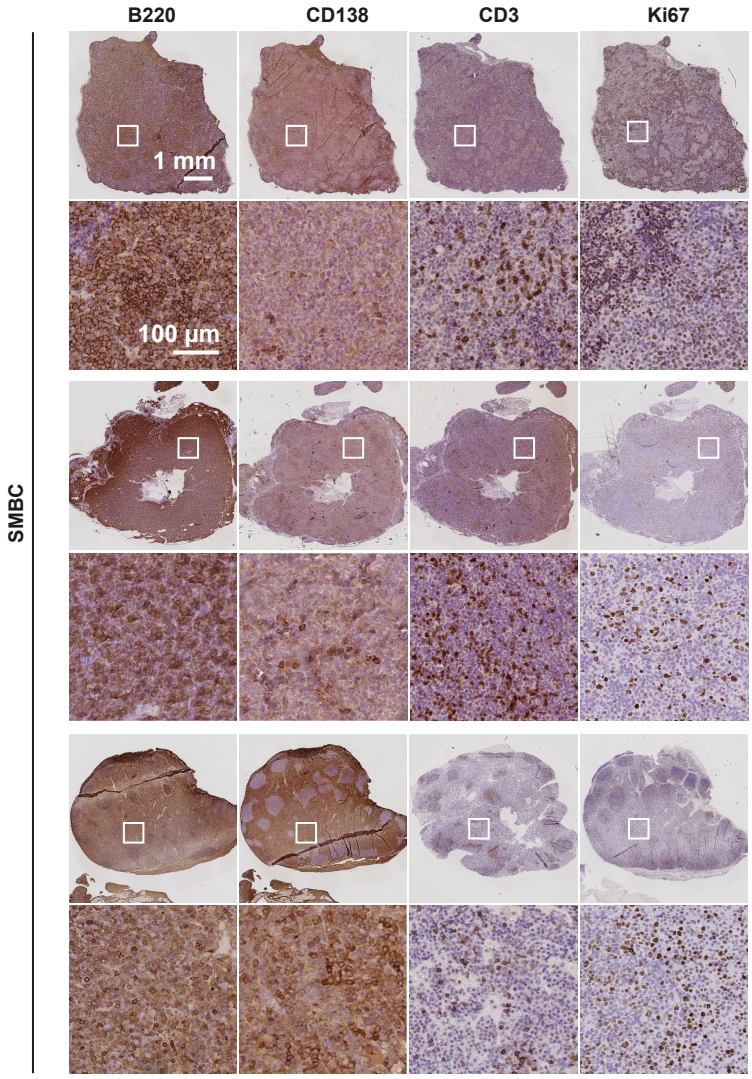

Supplementary Figure S4. Three representative immunohistochemical stainings of SMBC tumors (n = 16). The displayed staining patterns serve to illustrate the morphological and immunohistochemical bandwidth of analyzed SMBC lymphomas. Scale bars represent 1000 µm and 100 µm (low and high magnification, respectively).

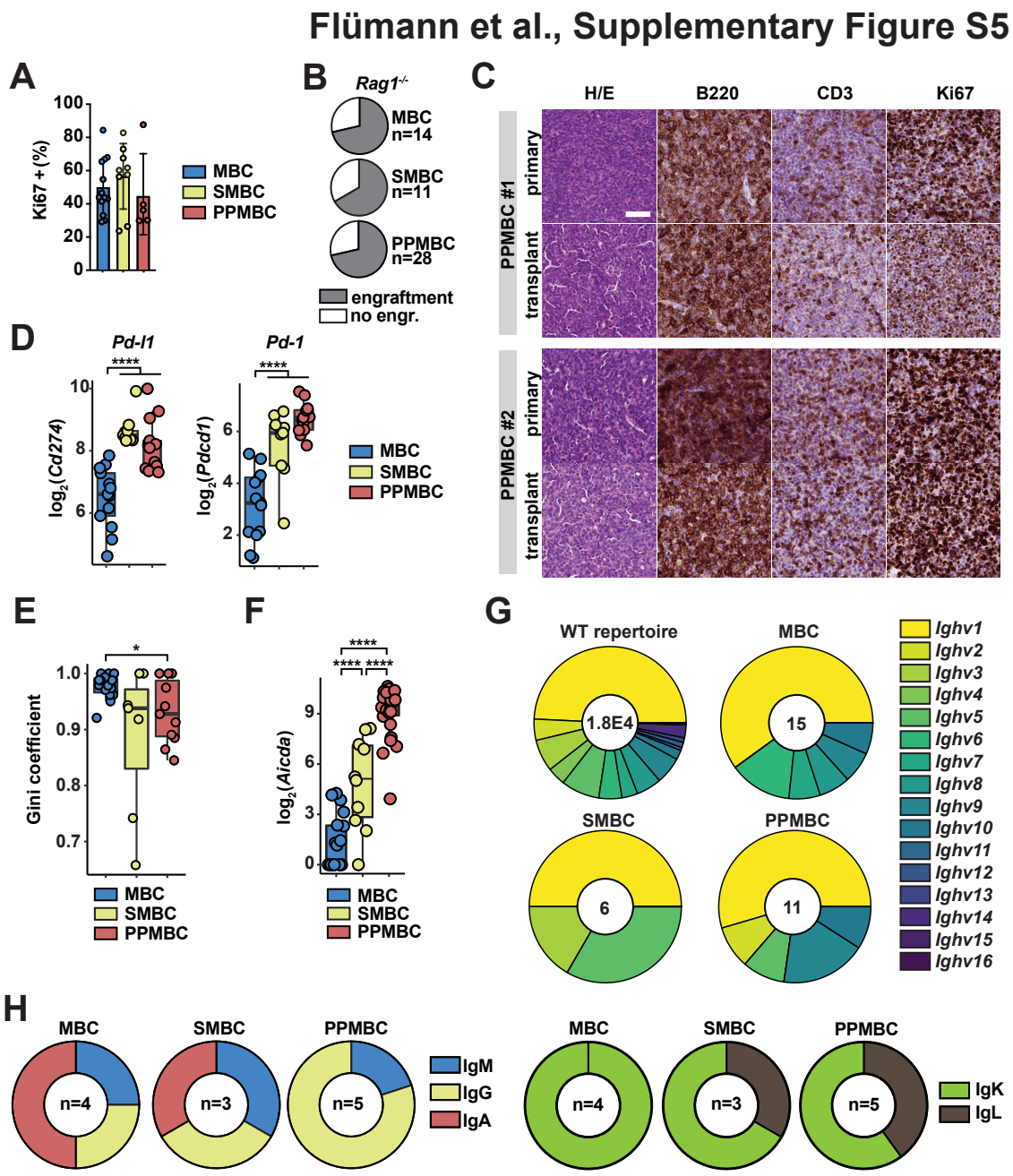

Supplementary Figure S5. **(A)** Quantification of Ki67⁺ cells in IHC stainings of MBC (n = 13), SMBC (n = 9) and PPMBC (n = 5) lesions. **(B)** Engraftment efficiency of MBC, SMBC and PPMBC lymphomas in *Rag1*$^{-/-}$ mice. **(C)** IHC stainings of two transplanted primary lymphomas and their respective engrafted tumors in immunocompetent recipient mice. Scale bar represents 50 µm. **(D)** Transcription levels of *Cd274* and *Pdcd1* (a.k.a. *Pd-l1* and *Pd-1*, respectively) in MBC, SMBC and PPMBC lymphomas. **(E)** Gini coefficients indicating the size distribution between individual subclones within the largest cluster of a given tumor. **(F)** Transcription levels of *Aicda* in MBC, SMBC and PPMBC lymphomas. **(G)** Visualization of the V_H family usage in MBC, SMBC and

PPMBC malignant clones. Numbers in the circles represent the number of clones analyzed for each genotype. For the tumor sample, each clone was derived from an independent lymphoma. For the WT repertoire, all clones of three independent spleen samples were pooled, while for lymphoma samples only the dominant clone of each sample was analyzed. **(H)** Quantification of the isotype usage (heavy and light chain) of malignant clones from the indicated number of lymphoma samples. *, $p \leq 0.05$; **, $p \leq 0.01$; ***, $p \leq 0.001$; Welch's unpaired two-tailed t-test; error bars represent SD.

Flümann et al., Supplementary Figure S6

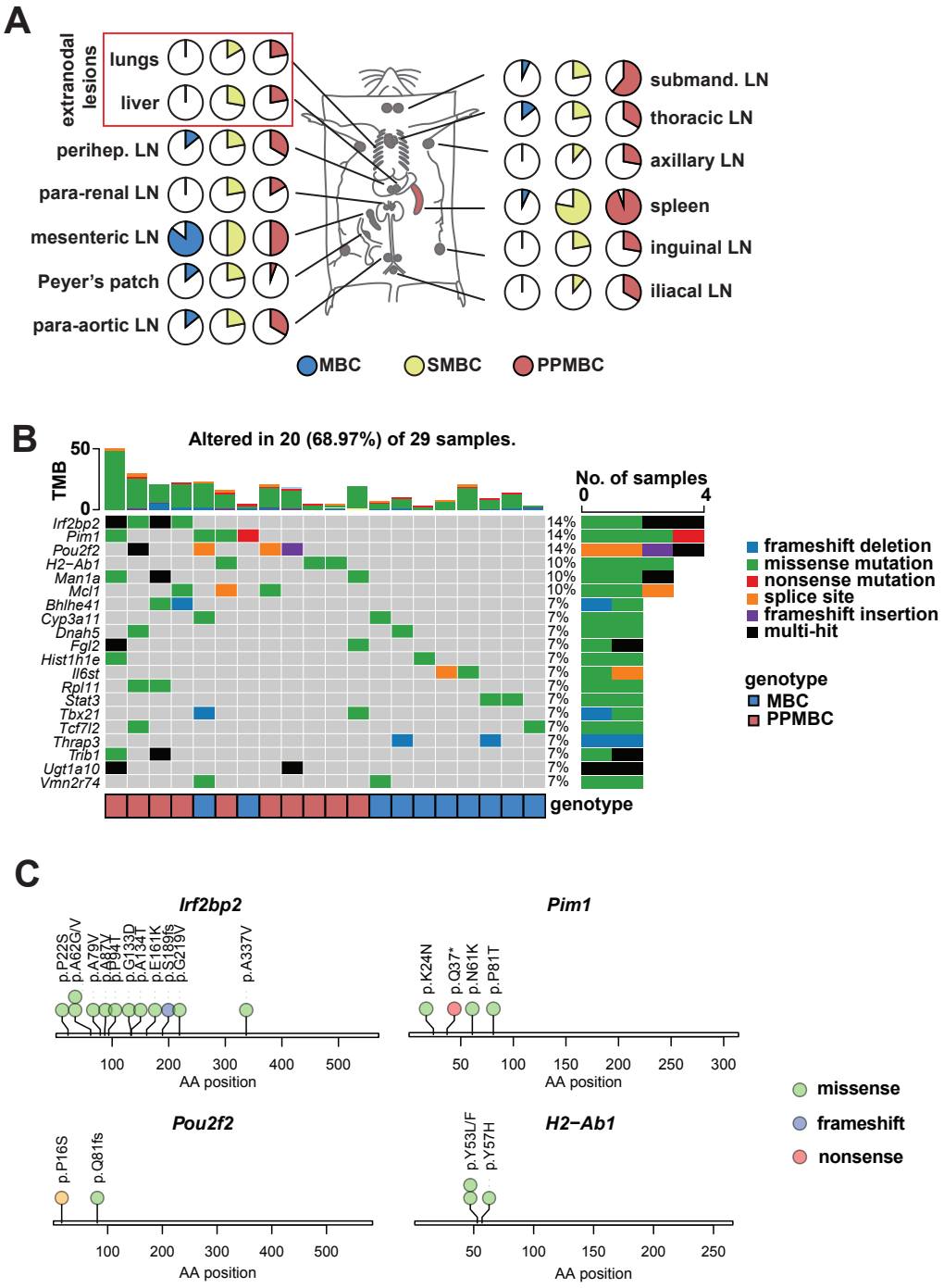

Supplementary Figure S6. (A) Genotype-specific quantification of involved lymph node ('LN') sites in the analyzed cohorts (MBC, n = 14; PPMBC, n = 15; SMBC, n = 10). **(B)** Oncoplot of a WES dataset generated from MBC (n = 17) and PPMBC (n = 12) tumors. **(C)** Lollipop plots for recurrently mutated genes. Numbers on x axis indicate the position on the cDNA sequence.

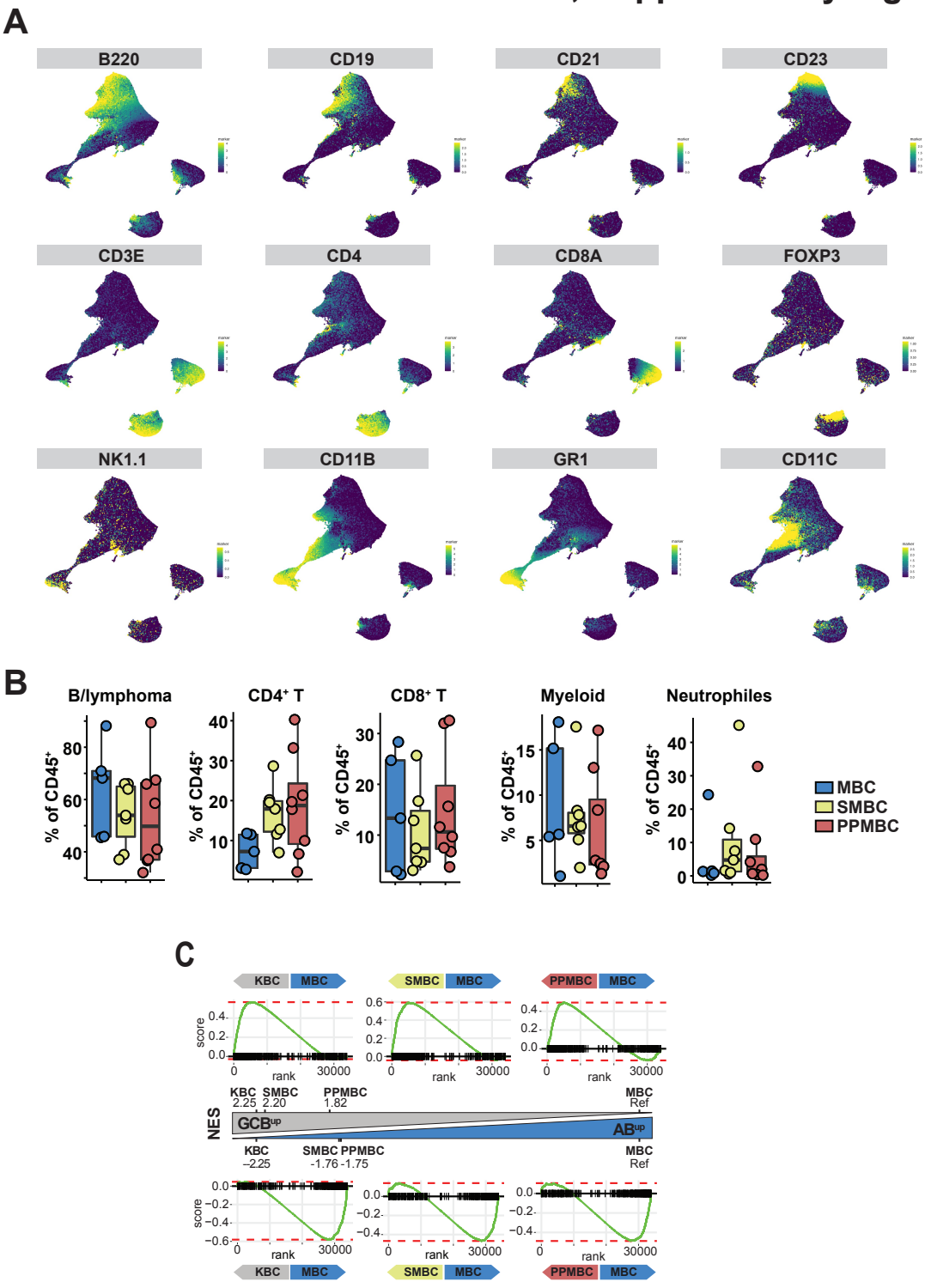

Supplementary Figure S7. (A) UMAP plots corresponding to **Fig. 3A** with the signal intensities of all markers used for dimensionality reduction visualized by color scale. **(B)** Cluster sizes observed in MBC (n = 5), SMBC (n = 7) and PPMBC (n = 8) samples. **(C)** Gene set enrichment plots comparing MBC, SMBC and PPMBC to the KBC model as reference. The normalized enrichment score (NES) is illustrated as an

approximation of distance between the genotypes. AB, “activated B”; GCB, “germinal center B”.

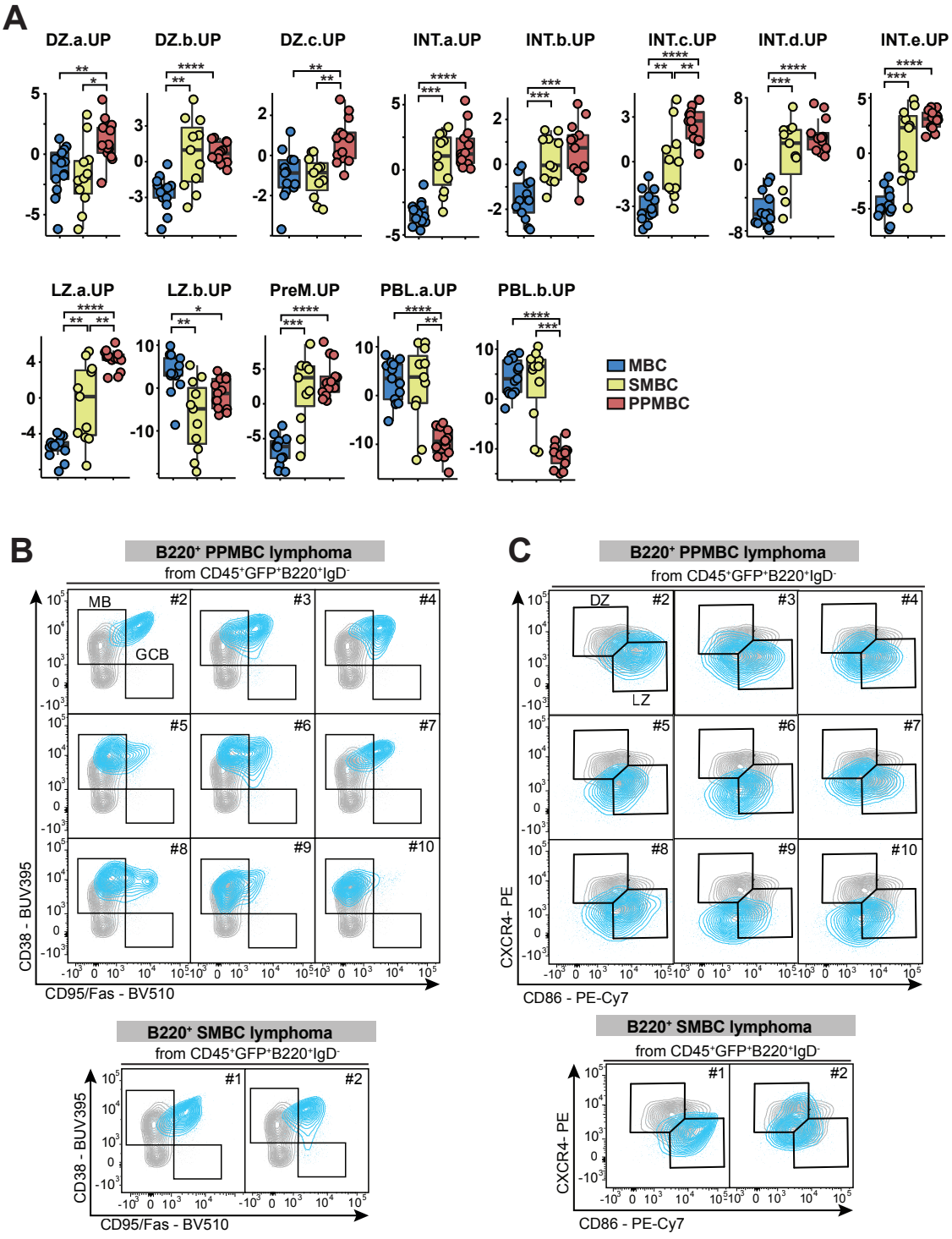

Supplementary Figure S8. (A) Visualization of ssGSEA scores calculated for individual lymphoma samples for each of the indicated gene sets derived. **(B, C)**: Contour plots showing staining pattern of CD38 and CD95/Fas **(B)** or CXCR4 and CD86 **(C)** in B220^{pos} PPMBC and SMBC lymphomas (blue) as overlay over splenic B220+ IgD- cells **(B)** or GCB cells **(C)** from a healthy control mouse (light grey). The

numbers indicate case numbers and are corresponding between **(B)** and **(C)**. *, p ≤ 0.05; **, p ≤ 0.01; ***, p ≤ 0.001; Welch's unpaired two-tailed t-test.

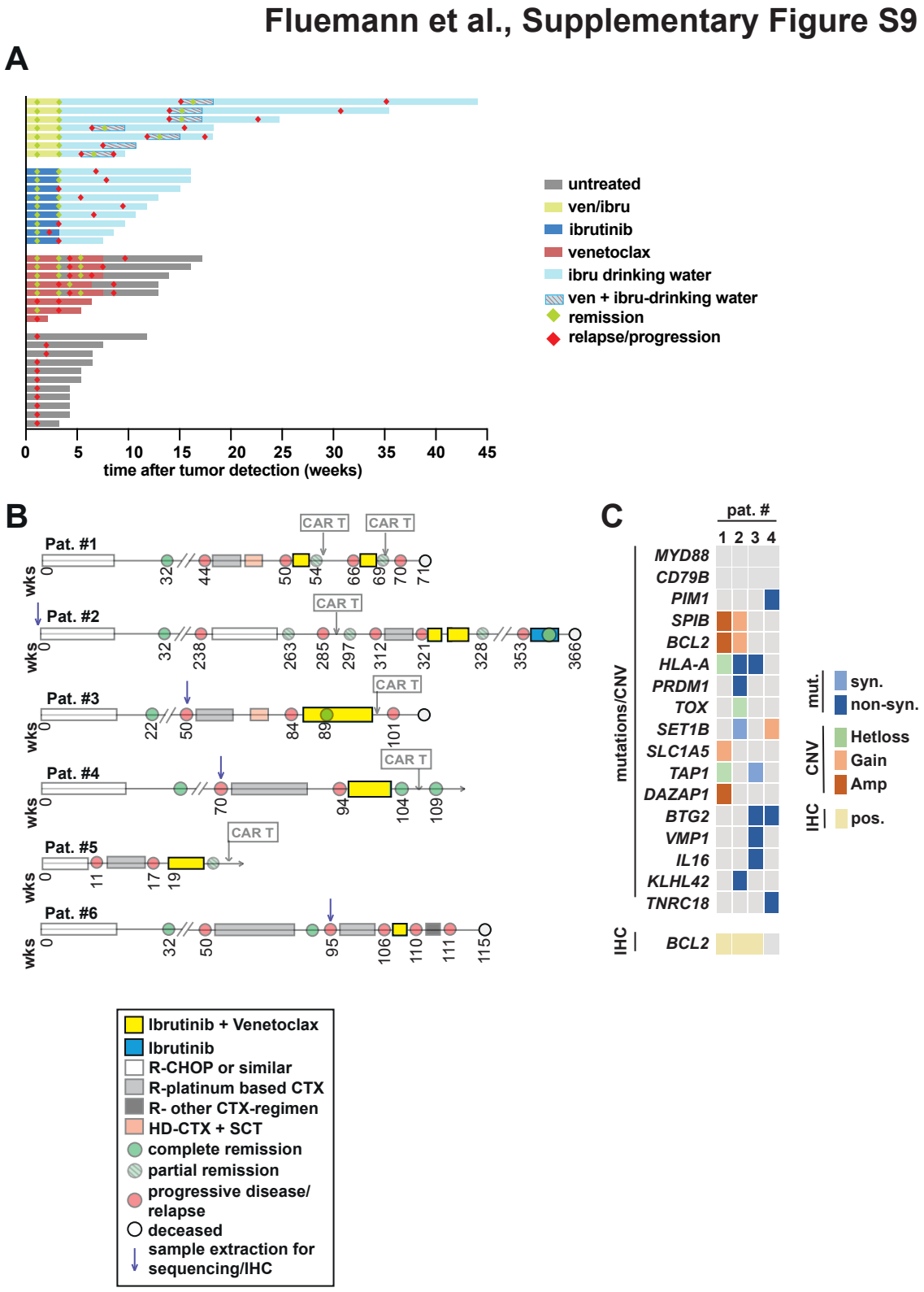

Supplementary Figure S9. (A) Swimmer's plot of treatment duration, response, and

outcome of treated mice. **(B)** Detailed treatment history of the investigated patients (wks; weeks). **(C)** Oncoplot for genetic features significantly associated with the MCD cluster and BCL2 status according to IHC for each patient.

Fluemann et al., Supplementary Figure S10

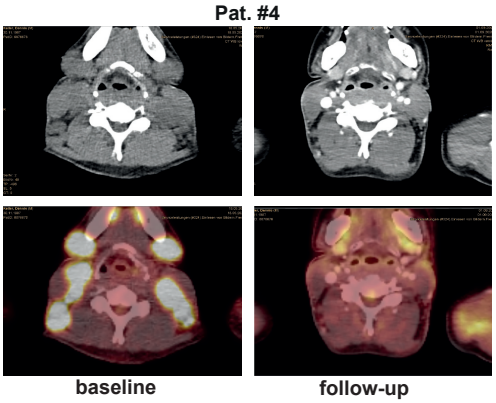

Supplementary Figure S10. Baseline and follow-up PET-CT of Patient #4.

Fluemann et al., Supplementary Figure S11

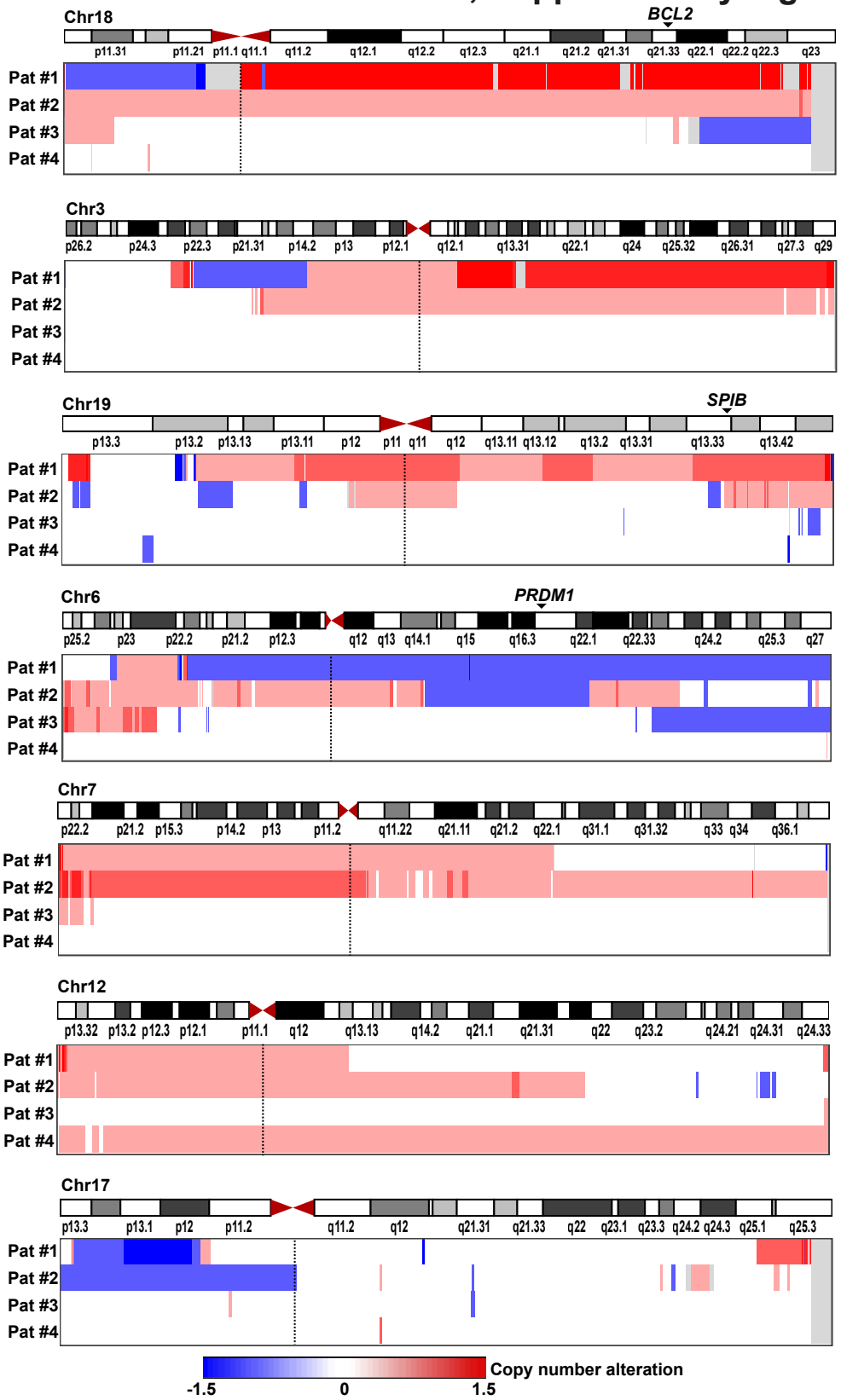

Supplementary Figure S11. Copy number profiles of chromosomes recurrently affected by arm-wise alterations in DLBCL.

Fluemann et al., Supplementary Fig. S12

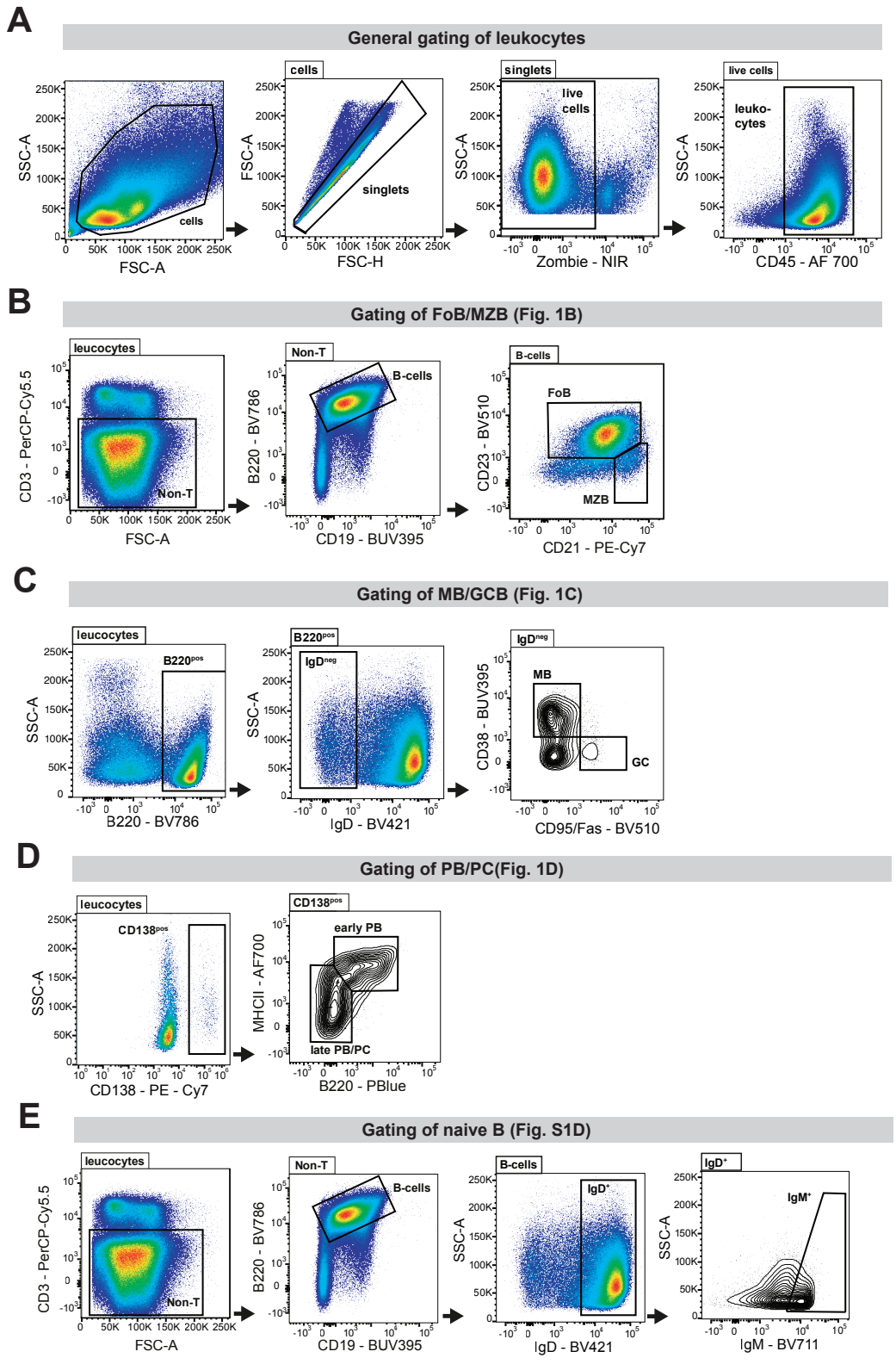

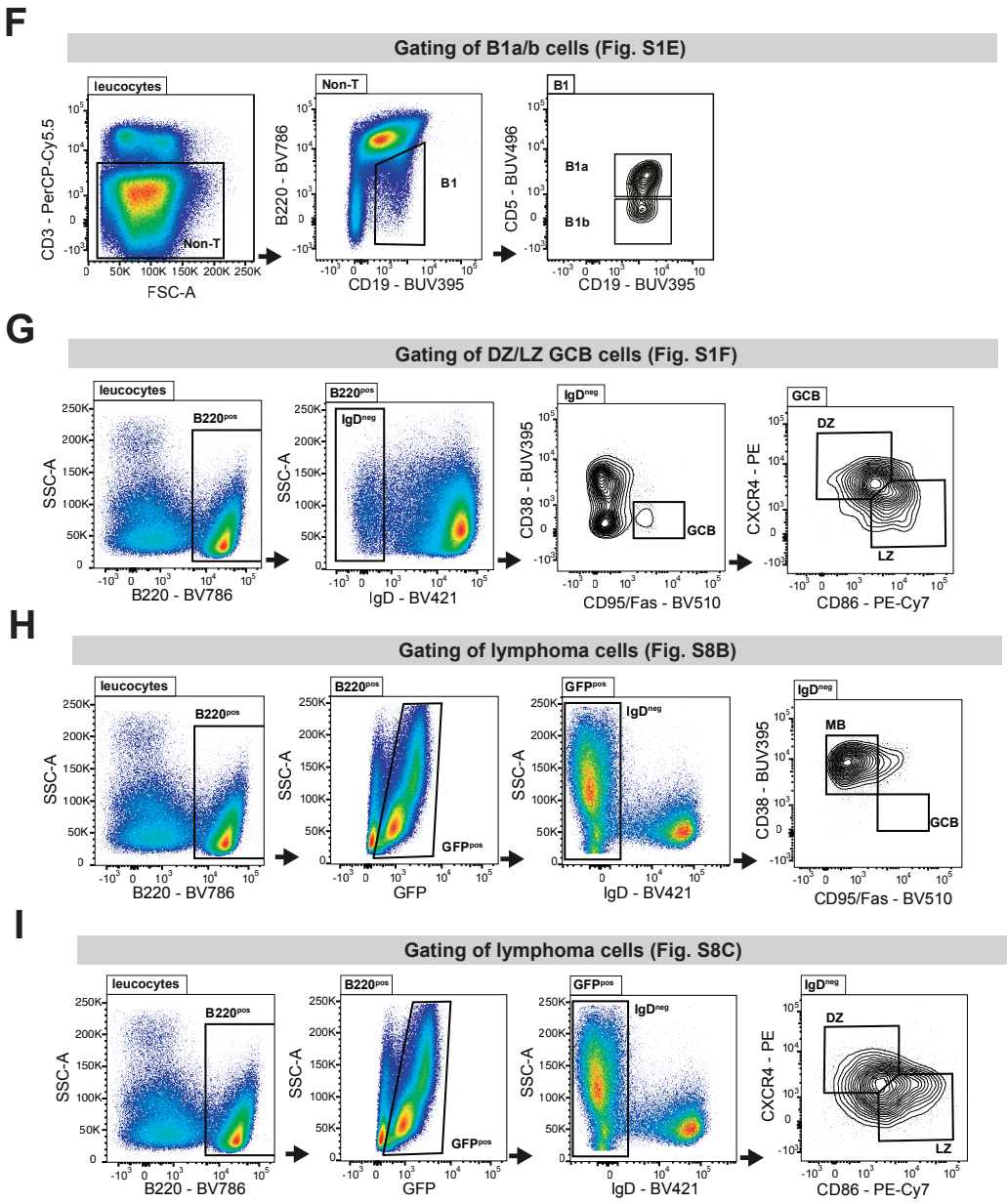

Supplementary Figure S12: Depiction of the full gating strategies used for the indicated analyses. **(A)** visualizes the general strategy for single cell leukocyte events that is upstream of the gating strategies illustrated in **(B)** to **(I)**.